E3: Hysteresis Loops

Andrew Norman, Pembroke College

Michaelmas term, 2007

Experiment performed Friday 2nd and Monday 5th November, 2007

Abstract

An account is given of experiments to measure magnetic hysteresis curves of mild steel, transformer iron and a copper-nickel alloy. The $B - H$ characteristics of samples of these materials are plotted, and the ranges of μ_r and an estimation of the energy loss during a hysteresis cycle are given. A discussion of how the measured properties of transformer iron are appropriate to its function follows. The hysteresis property of the copper-nickel alloy was found to disappear above its Curie temperature, though we were unable to accurately determine the transition temperature. The limitations of the methods used are discussed, with some suggestions with regard to their improvement, and the results obtained are compared to those of theory.

1 Introduction

Ferromagnetic materials become magnetized when subjected to a magnetic field, and this magnetization persists when the field is removed. This irreversibility of the magnetization and demagnetization process is termed *magnetic hysteresis*, and is an important phenomenon. The properties of ferromagnetic materials in relatively low magnetic fields, epitomized in the hysteresis loop, have been the subject of extensive theoretical and experimental investigation. In this experiment, we aim to measure the hysteresis curves of a number of ferromagnetic materials, as an example of non-linearity due do irreversible microscopic processes, and to investigate the behaviour of a material as it loses its hysteresis properties above the Curie temerature.

2 Background & Theory

The only elements which exhibit ferromagnetism at room temerature are iron, cobalt, nickel and gadolinium [11], since the atoms of these elements contain unpaired electrons and their atomic structure allows the cooperative parallel alignment of the magnetic dipole moments. Within a ferromagnetic material, there are regions in which the magnetic dipole moments are aligned in the same direction, called domains, each with an overall magnetic moment. In a demagnetized sample, the domain moments are pointing at random, and so the overall magnetic dipole moment of the material in any direction is zero. When the material is magnetized the vector summation of the dipoles in the domains gives an overall magnetic dipole.

As an unmagnetized sample of a ferromagnetic material is subjected to an increasing magnetic field, domains with magnetic moments in the closest directions to that of the applied field grow at the expense of others, through motion of the domain walls. The initial small movement of domain walls is reversible, and if the applied field is removed the magnetization will return to the initial demagnetized state. In this region the magnetization curve is reversible and therefore does not show hysteresis.

As the domain walls continue to move, they will encounter defects in the crystal structure, and require energy to move past these (provided by the applied magnetic field), making it more difficult to magnetize the sample. As the domain moves past the imperfection, there is a sharp change in the magnetic flux, which can be detected as crackling in a speaker connected via an amplifier to a coil wound around the specimen. This phenomenon is known as the Barkhausen effect [9], and it shows that the magnetization is made up of small discontinuous and irreversible changes (so the magnetization 'curve' is in fact a series of steps).

Eventually domains with dipole moments pointing along the easy axis closest to the direction of the applied magnetic field will dominate the sample, ultimately forming one homogeneous domain. Further increase in magnetization can only occur by the dipole moment of this domain rotating away from the easy direction to an orientation parallel to that of the externally applied field, and once this has happened, the material has reached its saturation magnetization. This final rotation can be quite difficult, depending on the properties of the material, and generally leads to further non-linearity of μ in this part of the magnetization curve.

Above a critical temperature, T_C, all materials become paramagnetic (i.e. with no field the magnetic moments are randomly orientated due to thermal fluctuations, and the magnetization is directly proportional to the applied field, with μ_r being constant), since thermal energy is large enough to over-

come the energetic advantage of magnetic ordering.

Due to the fact that ferromagnetic materials can be 'poled' by an applied field, and they store their remanent magnetization even when the field is removed (the hysteretic property), they have important applications in the storage of information in computer memory.

A ferromagnetic material with some remanent polarization once the field has been removed contains energy, since work has been done in magnetizing it [4]. The work done w_m in magnetizing a sample to saturation when it is initially unmagnetized, is given by

$$w_m = \int_0^B H \ dB,$$

i.e. the area between the curve and the B axis gives the energy density. If a hysteresis loop is traced out, the area enclosed gives the energy lost (expended as heat, or in setting up eddy currents) in one complete cycle.

3 Methods

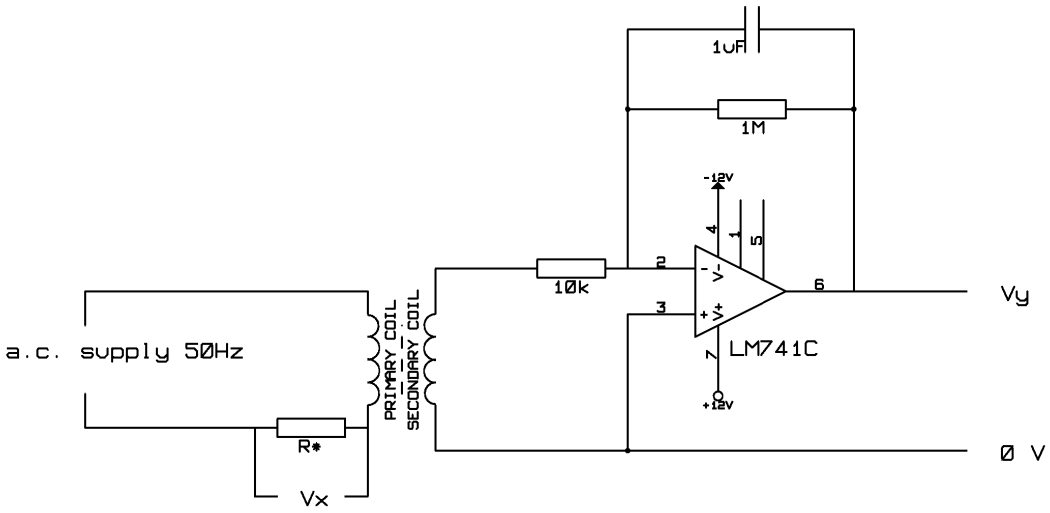

Figure 1: The circuit. V_x and V_y were displayed on the X and Y channels of a cathode ray oscilloscope (CRO), using $\times 10$ probes, and X-Y coupling was used to display the hysteresis curves.

3.1 H field inside primary coil

For a long solenoid (in this case the primary coil, with a core of relative permeability μ_r) length l with N turns and carrying current I, the magnetic field strength B along the centre is given by

$$B = \frac{\mu_r \mu_0 N I}{l}.$$

We know that $H = B/\mu_r\mu_0$, and so we see that

$$H = \frac{NI}{l}.$$

Since $V_x = I_p R_*$ (see Figure 1) we can write

$$H = \frac{N_p}{l_p R_*} V_x. \tag{1}$$

3.2 B field with magnetization of core

For the secondary coil, we know from Faraday's law that

$$\varepsilon = -\frac{d}{dt}\ \Phi = -N_s A_s \frac{dB}{dt}$$

in this case. Therefore we see that

$$B = -\frac{1}{N_s A_s} \int \varepsilon dt.$$

We used a 741 operational amplifier (op-amp) as an integrating amplifier in our circuit (see Figure 1) and so

$$V_y = -\frac{1}{RC} \int \varepsilon dt,$$

where $R = 10\text{k}\Omega$ and $C = 1\mu\text{F}$ in our case. Equating $-\int \varepsilon dt$, we find $BN_sA_s = V_yRC$, and

$$B = \frac{RC}{N_s A_s}\ V_y \tag{2}$$

3.2.1 The Integrator

We set up an integrating amplifier, as described above, to be responsive at frequencies of around 50 Hz. We needed the capacitor's impedance to be much lower than that of the resistor (1MΩ) at this frequency, without driving the gain down to a really tiny value (Gain = $\frac{1}{\omega RC}$). We measured the properties of the components used using a bridge provided in the IB Class, and calculated the gain to be 0.32 ± 0.02 when measured on the oscilloscope, this turned out to be 0.43 ± 0.02. We suspect that there was some sytematic error in the bridge which was used to measure the component values used to compute the 'theoretical' value for the gain. We also checked that the input voltage form was integrated before being passed to the output by using X-Y coupling on the oscilloscope. When the input (sinusoidal) and output voltages were applied to the X and Y channels respectively, an ellipse was produced, showing that the output was $\frac{\pi}{2}$ out of phase from the input. The displayed traces in DUAL display confirmed that integration was occuring.

3.3 Calibration

It was expected (see above) that

$$V_x = \frac{R_* l_p}{N_p} \frac{B}{\mu_r \mu_0}$$

and

$$V_y = \frac{N_s A_s}{RC} B.$$

We see that

$$\frac{V_y}{V_x} = \frac{N_p N_s A_s \mu_0}{RC R_* l_p} \mu_r$$

The equipment was calibrated using an air core, with μ_r presumed to be 1 (quoted as 1.0005 in [10]). All of the necessary constants were measured, and V_y/V_x was calculated to be 0.017 ± 0.001. The measured value turned out to be 0.0113 ± 0.0004, and so was not in agreement to within the estimated errors.

We identified a number of sources of error on this measurement:

1. There could have been stray resistances or capacitances on the bread-board and in the wires.

2. R_* was a small resistance, and so a small error here would lead to a larger percentage error in the final result. We tried to alleviate this, however, by making sure the multimeter read zero with zero resistance,

and allowing the resistor to heat up to its operating temperature before measuring it.

3. The measurement of area had quite a large uncertainty, since we could only measure the external diameter of the former. We measured this diameter in several orientations to get a more accurate value.

4. The field probably was not entirely uniform within the primary coil. We found that V_y/V_x varied as the secondary coil was moved inside the primary coil, and we adjusted its height so as to maximize V_y/V_x.

5. There would have been some leakage of flux out of the ends of the coil, since it is not an infinite solenoid as we have presumed in our treatment (see Discussion).

3.4 Plotting the data

In order to turn the V_y vs. V_x plot (read off from the CRO screen) into a $B - H$ characteristic, we needed to obtain the constants of proportionality as described in *Methods*.

Quantity	Method of measurement	Value obtained
l_p	Steel rule	(18.0 ± 1.0) mm
R_*	Digital multimeter	(2.5 ± 0.1) Ω
N_s	Quoted on component	500 ± 1
N_p	Quoted on component	400 ± 1
R	Bridge	(9.951 ± 0.001) Ω
C	Bridge	(735.2 ± 0.1) μF

The area A_s was taken as the area of the core only (when the core was not air), since the core materials used had $\mu_r \gg 1$, and so almost all of the magnetic flux inside the secondary coil would be passing through them. This simplification was a source of systematic error.

The areas of the cores were found to be

Air	$(22.66 \pm 0.12) \times 10^{-6}$ m^2
Mild Steel	$(8.24 \pm 0.05) \times 10^{-6}$ m^2
Transformer Iron	$(2.85 \pm 0.04) \times 10^{-6}$ m^2
CuNi alloy	$(19.95 \pm 0.08) \times 10^{-6}$ m^2

4 Results

See Figures 2 - 4 for the hysteresis plots.

	Energy loss / Jm^{-3}	Lowest μ_r	Highest μ_r	$\triangle\mu_r$
Mild Steel	72 000 ± 1 000	8.5 ± 0.5	57 ± 4	39 ± 4
Transformer Iron	26 400 ± 1 000	9.4 ± 0.6	143 ± 9	134.5 ± 9
CuNi alloy below 40 °C	1 540 ± 30	0.86 ± 0.01	15.3 ± 0.2	14.4 ± 0.2
CuNi alloy above 40 °C	< 10	0.81 ± 0.01	0.81 ± 0.01	< 0.02

Values of μ_r were obtained by using gradient triangles on the $B - H$ plots, and the areas of the hysteresis curves were estimated by a summation of polygon areas to calculate the energy lost in hysteresis.

5 Discussion

In transformers and motors, magnetic materials are subjected to rapidly alternating magnetic fields, and the hysteresis cycle is repeated (at 50 Hz in the case of transformers at the normal power supply frequency). This hysteresis loss leads to a reduction in efficiency and adds to the temperature rise produced in the equipment, so for such applications materials of low hysteresis loss are required. If saturation occurs in transformers, the waveform of the output current will not follow the waveform of the input current [6]. We see from our results that transformer iron has a low energy loss (compared to mild steel). Although the CuNi alloy has a lower energy loss per cycle, it also has a low μ_r which would make it quite unsuitable for use in a transformer core, which needs to be soft, so that a large magnetization results from a small applied field.

No hysteresis was seen in the copper-nickel alloy above 40 °C, and we conclude that this is above its Curie temperature, and it has become paramagnetic. Our results show, however, that $\mu_r = 0.81$, suggesting that χ_m, the magnetic susceptibility, is negative i.e. the material is diamagnetic. This contradicts the accepted body of evidence [11] and so we should suggest that this discrepancy points to a hitherto unnoticed error in our approach.

The technique which we used would not lend itself to measuring the hysteresis properties accurately close to T_C for the copper-nickel alloy, since the temperature could not be controlled or measured accurately enough. A major problem was the self heating of the outer coil, and an experiment to investigate property variation with temperature would need to have insulation so that the outer coil would affect the sample (within the secondary coil)

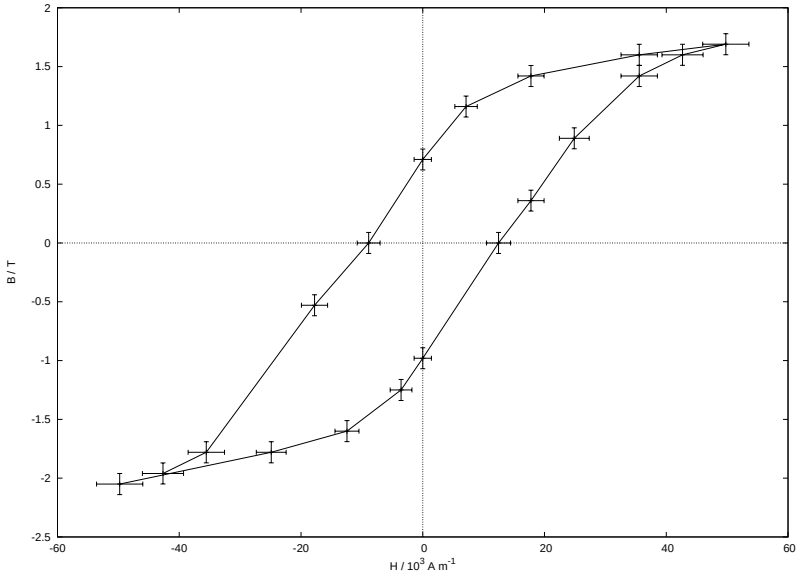

Figure 2: **Mild steel** The B and H axes were calibrated as described in *Methods*. Note, however, that the zero axes do not represent zero B or H fields, due to a D.C. offset in the experiment.

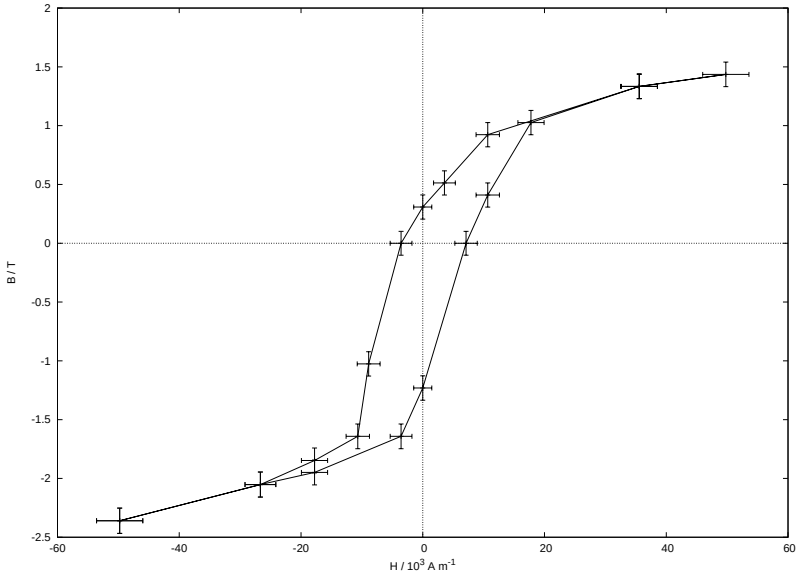

Figure 3: **Transformer iron** Again, the D.C. offset causes the zero axes on the graph not to correspond to zero B and H fields.

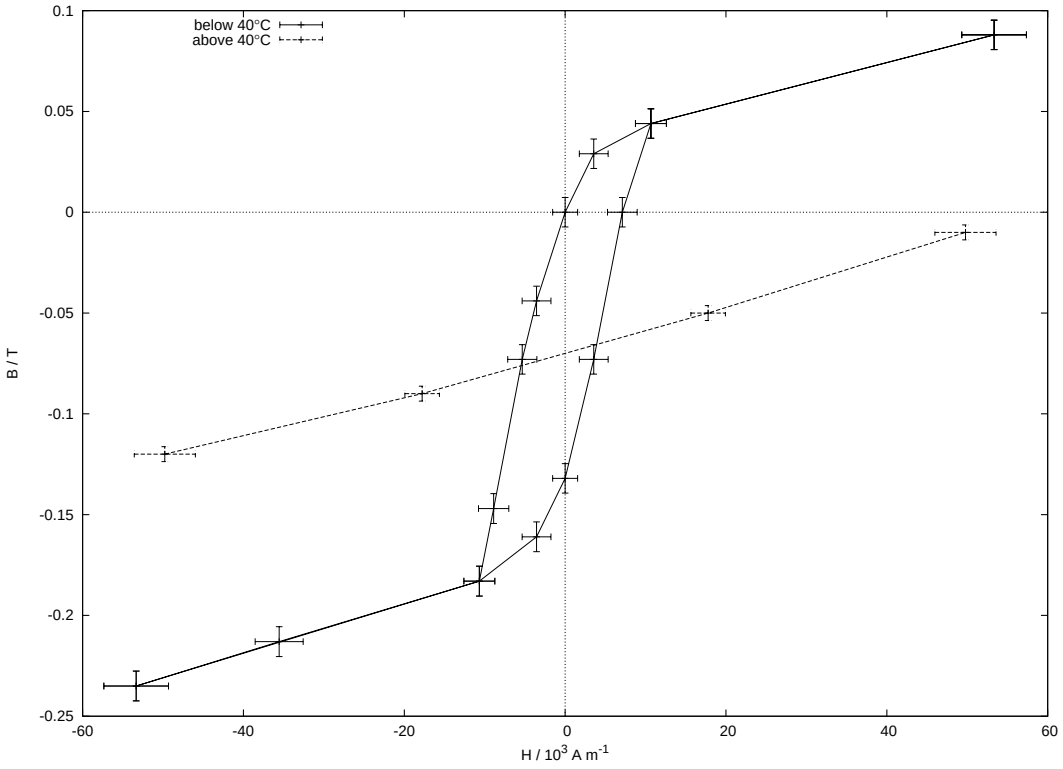

Figure 4: Copper-Nickel alloy characteristics both above and below 40 °C. As T decreases, the loop area increases, as more energy is needed to re-orientate the domains which are "frozen in." Above T_C the material is paramagnetic and has constant μ_r.

magnetically but not thermally. A better system would also be needed for measurement of temperature (e.g. a sensor inside the secondary coil).

In our experimental setup, we had some leakage of flux at the ends of the coil. This could have been massively reduced using a toroidal coil, with no demagnetizing field at the 'free poles' (as desribed in [7], section 6.8).

6 Conclusions

1. Hysteresis was observed in a variety of ferromagnetic materials, and their individual properties were linked to their applications as materials.

2. The loss of hysteresis above the Curie temperature was observed for a copper-nickel alloy. This is a general property of ferromagnets. Note, however that we observed diamagnetism rather than paramagnetism.

References

[1] Cavendish Laboratory: *IB Physics A & Physics B Practicals: Systems and Measurement*, Michaelmas 2007

[2] F. Brailsford: *Magnetic Materials*, Methuen, 3rd ed., 1960

[3] Richard P. Feynman: *The Feynman Lectures on Physics, Volume II*, Addison-Wesley, 1964

[4] John D. Kraus: *Electromagnetics*, McGraw-Hill, 4th ed., 1992

[5] Dr. Judith Driscoll: *Course C: Materials and Devices*, Materials and Minerals Sciences, University of Cambridge, 2006

[6] Prof. S. Withington: *Electromagnetism Lecture Notes*, Department of Physics, University of Cambridge, 2007

[7] Bleaney, B.I. & Bleaney, B.: *Electricity and Magnetism*, Oxford University Press, 1991

[8] R S Tebble et al. *Proc. Phys. Soc. A* **63** No 7 (1 July 1950) 739-761

[9] R S Tebble *Proc. Phys. Soc. B* **68** No 12 (1 December 1955) 1017-1032

[10] M Fujihira *Annual Review of Materials Science, 1999* Vol. 29 353-380

[11] DoITPoMS: *Teaching and Learning Packages*, Department of Materials Science and Metallurgy, University of Cambridge (see http://www.doitpoms.ac.uk)

Typeset using LaTeX.
Graphs plotted with Openoffice.org, GNU Emacs, gnuplot and EPSTOPDF.
Circuit diagram produced using EESchema and EPSTOPDF.